

Table 3 (cont.)

	Z	a	b	c	ϵ (%)
Ac	89	1.0137	0.5648	1.5024	0.3088
Th	90	1.0110	0.5655	1.4917	0.3069
Pa	91	1.0135	0.5479	1.5279	0.3102
U	92	1.0184	0.5884	1.4479	0.3423
Np	93	1.0161	0.5407	1.5358	0.2950
Pu	94	1.0150	0.4812	1.6715	0.3230
Am	95	1.0162	0.4605	1.7288	0.3042

used with universal parameters, independently of the atomic species. The accurate values of Cromer (calculated from HF-SCF wave functions, based on the complete W-H theory) can be approximated by the analogue expression (5) with the individual parameters tabulated in Table 3. Neither of the fits depends on the atomic form factors.

As to the mean errors of the latter fits, they are of the same order of magnitude as those of the squares of the published analytic fits for the form factors. Thus both the coherent and the incoherent terms contribute equally to the error of the total scattered intensities. Weighting of the deviations by s was meant to enhance the accuracy of the fit with growing s in order to keep the error of the approximated total scattered intensities on a standard level.

The limiting value of the analytic expression for $s=0$ is $1-a$. It is seen from Table 3 that the parameter a is by 0.5–6% over unity. Although fixing it as $\equiv 1$ would result in zero for $I_{inc}(0)$, the remaining two parameters would yield a poorer fit. From Table 2, it is seen that the fit is not very good below $s=0.1$. This inaccuracy is not significant for total scattered X-ray intensities, the contribution of the incoherent part being negligible in this range. However, the same cannot be stated of electron scattering, and therefore the use of our formula for deriving differential inelastic electron scatter-

ing factors in this range would lead to insufficient results.

The author wishes to thank Professor Dr S. Lengyel and Mr F. Hajdu for the discussion of the manuscript and Mrs M. Kovács for her technical assistance. Calculations have been performed on the CDC 3300 computer of the Computing Centre of the Hungarian Academy of Sciences, Budapest.

References

- BEWILOGUA, L. (1931). *Phys. Z.* **32**, 740–744.
 CROMER, D. T. (1967). *J. Chem. Phys.* **47**, 1892–1893.
 CROMER, D. T. (1969). *J. Chem. Phys.* **50**, 4857–4859.
 CROMER, D. T., LARSON, A. C. & WABER, J. T. (1964). *Acta Cryst.* **17**, 1044–1050.
 CROMER, D. T. & MANN, J. B. (1968). *Acta Cryst.* **A24**, 321–324.
 CROMER, D. T. & WABER, J. T. (1965). *Acta Cryst.* **18**, 104–109.
 DOYLE, P. A. & TURNER, P. S. (1968). *Acta Cryst.* **A24**, 390–397.
 FREEMAN, A. J. (1959). *Acta Cryst.* **12**, 929–935.
 FREEMAN, A. J. (1960). *Acta Cryst.* **13**, 190–196.
 FREEMAN, A. J. & WATSON, R. E. (1962). *Acta Cryst.* **15**, 682–687.
 HAJDU, F. (1971). *Acta Cryst.* **A27**, 73–74.
 HAJDU, F. (1972). *Acta Cryst.* **A28**, 250–252.
 HANSON, H. P., HERMAN, F., LEE, J. D. & SKILLMANN, S. (1964). *Acta Cryst.* **17**, 1040–1043.
 MOORE, F. H. (1963). *Acta Cryst.* **16**, 1169–1175.
 PAKES, H. W. & LEE, J. D. (1969). *Acta Cryst.* **A25**, 712–713.
 POHLER, R. F. & HANSON, H. P. (1965). *J. Chem. Phys.* **42**, 2347–2352.
 TAVARD, C., NICOLAS, D. & ROUAULT, M. (1967). *J. Chim. Phys.* **64**, 540–554.
 THOMAS, L. H. & UMEDA, K. (1957). *J. Chem. Phys.* **26**, 293–303.
 TIETZ, T. (1959). *Phys. Rev.* **113**, 1521–1522.

Acta Cryst. (1973). **A29**, 12

X-Ray Diffraction Profiles of Defective Layered Lattices Showing Preferred Orientation

BY SABRI ERGUN AND MARTIN BERMAN

Spectro-Physics, Pittsburgh Energy Research Center, U.S. Bureau of Mines, Pittsburgh, Pennsylvania 15213, U.S.A.

(Received 9 June 1972; accepted 31 July 1972)

In layered lattices the layers tend to stratify and the stratified layer domains often exhibit preferred orientation in bulk samples. Using the Laplace and Hankel transform techniques, equations have been developed for the profiles of the two-dimensional (hk) reflections from defective layered lattices in different orientation modes. Two different approaches have been used in the derivation, the inter-atomic distance sum method and the lattice sum method, and the results have been compared.

Introduction

In explaining the linewidths of diffraction patterns, the concept of coherently scattering crystallites as domains

has been found to be convenient. The particle size concept has been well entrenched in spite of recognition (Warren, 1959) that the materials studied in most instances are not fragmented into small separate par-

ticles of sizes indicated by the linewidths. The treatment presented below is based on the theory of defective lattices (Ergun, 1970a). According to the theory, diffusely scattering substances are essentially highly defective lattices rather than made up of small incoherently scattering crystallites. Fig. 1 shows a model of defective lattices using a raft of bubbles (Bragg & Nye, 1947). It is seen that the concept of a defective lattice is amenable to illustration, and, in such instances, it is physically more realistic and convenient to consider interdefect distances rather than domain sizes.

The case of layered lattices requires special attention (Warren, 1941) in that they tend to stratify and show preferred orientation. The profiles of the observed intensities depend upon the type as well as the degree of preferred orientation (Bacon, 1956; Ruland, 1967). In this paper we will confine our attention to the effects of the type of orientation. The effects of the degree of orientation will be given elsewhere (Ergun, in preparation).

Types of preferred orientation

The profiles of crystalline reflections are not significantly affected by the size of domains if the mean interdefect distance is less by a factor of five or more than the sizes of domains. We may therefore consider a sample to be made up of large defective domains. Their sizes and shapes are effectively studied by small-angle X-ray scattering or by electron microscope observations. In the case of layered structures these domains are characterized by a vector normal to the layers, *i.e.* along the direction of stratification. Three cases of preferred orientation are observed experimentally.

Case I. The normals of the domains are parallel

Samples of pyrolytic carbons and some polymers, *e.g.* polyethylene, are examples. They are best studied by placing the sample so that the diffraction vector makes a specific angle with the layer normals. If the diffraction vector is parallel, only the $00l$ reflections are observed. If it is perpendicular, only the $hk0$ reflections are observed. There is a specific angle for each of the hkl reflections, if they exist.

Case II. Normals of the domains lie in a circle

When drawn from a common point, the end points of the unit vectors describing the normals of the layer domains would lie on a circle on which the density of the end points would be constant. Fibers are examples of such a case. They are conveniently studied by placing a parallel bundle of fibers in such a manner that the diffraction vector makes a specific angle, ψ , with the axes of the fibers. The shapes and the intensities of the $hk0$ reflections would depend upon ψ (Ergun, 1970b). When $\psi=0$, only the $hk0$ reflections are observed. In this situation the profiles of the $hk0$ reflections are identical with those observed in Case I.

Case III. Random orientation

This is the case for the isotropic samples of layered structures.

In each of the three cases cited, the absence of the hkl reflections would indicate that the layers are random in rotation with respect to their normals and random in translation. The randomness is generally the rule rather than the exception in the case of carbon. Hence they are each cited as a prime example of random layered lattices.

The interference function

The interference function due to an interatomic distance vector \mathbf{l} is given by $\exp(i\mathbf{h} \cdot \mathbf{l})$ in which \mathbf{h} is the diffraction vector. The magnitude of \mathbf{h} is given by $h = 2\pi \sin \theta / \lambda$, 2θ being the scattering angle and λ the wavelength. We are interested in developing analytical expressions for the average value, $I(h, l)$, of $\exp(i\mathbf{h} \cdot \mathbf{l})$ for the different types of preferred orientations described above.

We may conveniently start with the case of circular rotation of the normals of layer domains in which the layers are random in rotation about their normals and random in translation. This situation is analogous to considering a layer parallel to an axis, rotating the layer about the axis and about its normal and translating along the axis. Let X be the axis, XY be the plane of the layer, and Z normal to the layer. Let ψ be the angle that the diffraction vector \mathbf{h} makes with the X axis, and β the angle that its projection on the YZ plane makes with the Z axis. The product of \mathbf{h} with the interatomic distance \mathbf{l} is given by

$$\mathbf{h} \cdot \mathbf{l} = hl (\cos \psi \cos \alpha + \sin \psi \sin \beta \sin \alpha) \quad (1)$$

where α is the angle between the X axis and \mathbf{l} . A cylindrical rotation about the X axis requires that β varies from 0 to 2π and random rotation of the layers requires that the angle α varies from 0 to 2π each with equal probability. The average value, $I(h, l)$, of $\exp(i\mathbf{h} \cdot \mathbf{l})$ while keeping ψ constant is given by

$$I(h, l) = \frac{1}{\pi^2} \int_0^\pi \int_0^\pi \exp(i\mathbf{h} \cdot \mathbf{l}) d\alpha d\beta \\ = J_0 \left(hl \cos^2 \frac{\psi}{2} \right) J_0 \left(hl \sin^2 \frac{\psi}{2} \right) \quad (2a)$$

where J_0 is the Bessel function of the first kind and of zero order.

$$\text{When } \psi = 0 \quad I(h, l) = J_0(hl) \quad (2b)$$

$$\text{When } \psi = \pi/2 \quad I(h, l) = J_0^2(hl/2) \quad (2c)$$

If the diffraction vectors were randomly oriented, the number of vectors making an angle between ψ and $\psi + d\psi$ with a pole would be proportional to $\sin \psi$. $I(h, l)$ would then take the form

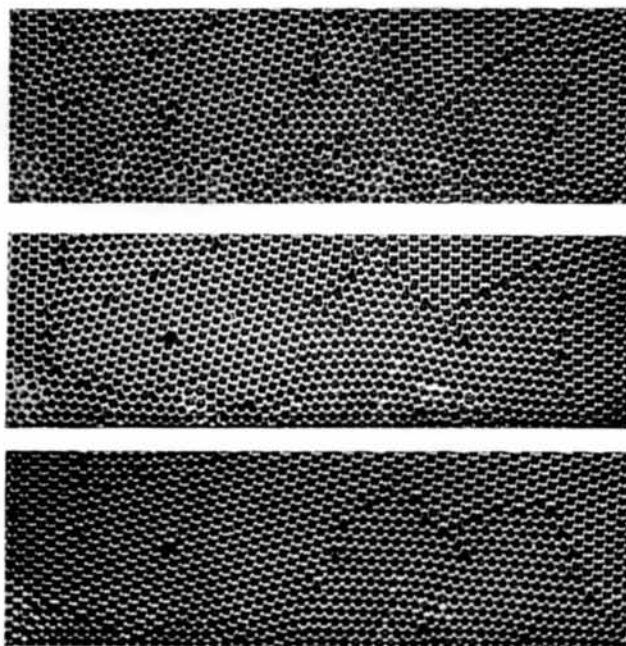


Fig. 1. Illustration of a defective lattice using a raft of bubbles (Bragg & Nye, 1947).

$$I(h, l) = \int_0^{\pi/2} J_0 \left(hl \cos^2 \frac{\psi}{2} \right) J_0 \left(hl \sin^2 \frac{\psi}{2} \right) \times \sin \psi d\psi = \sin(hl)/hl \quad (2d)$$

which is the well-known Debye interference function.

Equation (2b) may be directly obtained from

$$I(h, l) = \frac{1}{\pi} \int_0^{\pi} \exp(ihl \cos \alpha) d\alpha = J_0(hl),$$

and (2d) from

$$I(h, l) = \frac{1}{2} \int_0^{\pi} \exp(ihl \cos \alpha) \sin \alpha d\alpha = \sin(hl)/hl.$$

The atomic radial distribution method

For simplicity, consider a layered lattice containing one kind of atom and neglect the vibration and strain effects. The interference function, in atomic units, produced by a layer may be obtained from

$$j(h) = \int_0^{\infty} 2\pi r \rho(r) I(h, r) dr. \quad (3)$$

where $\rho(r)$ represents the average atomic density as a function of distance r from an atom. Thus $2\pi r \rho(r) dr$ gives the average number of atoms at a distance between r and $r + dr$.

Experimentally one obtains $j(h)$ and wishes to evaluate $\rho(r)$ using equation (3). To accomplish this, it is essential to develop an analytical expression for $I(h, r)$. Equations (2) furnish the desired analytical expressions. Cases I and II would permit experimentally placing the wave vector in the plane and the resulting interference function is given by equation (2b). For Case III we obtain the Debye interference function. Substituting equations (2b) and (2d) into (3) we obtain, respectively,

$$j(h) = \int_0^{\infty} 2\pi r \rho(r) J_0(hr) dr \quad (4b)$$

$$hj(h) = \int_0^{\infty} 2\pi r \rho(r) \sin(hr) dr. \quad (4d)$$

Equations (4b) and (4d) can be inverted using the Hankel and the Fourier inversion theorems respectively, and we obtain

$$2\pi r \rho(r) = r \int_0^{\infty} hj(h) J_0(hr) dh. \quad (5b)$$

$$2\pi r \rho(r) = \frac{1}{\pi} \int_0^{\infty} hj(h) \sin(hr) dh. \quad (5d)$$

Equation (5b) does not seem to have been used to date in structural analysis. Analysis of the structure from the intensity profiles obtained in the oriented state has tremendous advantages over those obtained in the random state (Ergun, 1970b).

Interatomic distance sum method

If we were to consider all of the interatomic distances, the interference function $j(h)$ would take the form

$$j(h) = \sum_{l=0}^{\infty} n(l) I(h, l) \quad (6)$$

where $n(l)$ is the number of neighboring atoms at a distance l from any atom. The variables n and l characterize the structure. Equations for n and l can be formulated for any lattice of infinite extent (Ergun, 1970a, c). In a domain of finite extent or in defective lattices, $n(l)$ is less than that which exists in a lattice of infinite extent. We may modify $n(l)$ by a function $g(l)$ properly chosen to account for both the shape and size effects. For very defective lattices $g(l)$ is given by

$$g(l) = \exp(-l/R) = \exp(-al) \quad (7)$$

$$a = 1/R$$

where $2R$ is the mean interdefect distance, *i.e.* starting from any atom the probability of traversing a distance R irrespective of direction, without encountering a defect is $1/e$. Substitution of equations (7) and (2) into (6) yields

$$j(h) = \sum \exp(-al_q) n(l_q) \times J_0 \left(hl_q \cos^2 \frac{\psi}{2} \right) J_0 \left(hl_q \sin^2 \frac{\psi}{2} \right) \quad (8a)$$

$$j(h) = \sum \exp(-al_q) n(l_q) J_0(hl_q) \quad (8b)$$

$$j(h) = \sum \exp(-al_q) n(l_q) J_0^2(hl_q/2) \quad (8c)$$

$$j(h) = \sum \exp(-al_q) n(l_q) \sin(hl_q)/hl_q. \quad (8d)$$

If $2R < 30 \text{ \AA}$, equations (8) can effectively be used to calculate the intensity profiles using a computer. Calculated profiles using equations (8b–8d) are shown in Fig. 2. The results correspond to the two-dimensional

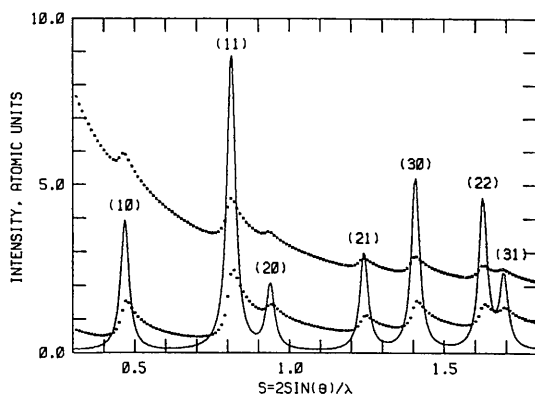


Fig. 2. Effect of orientation on the intensities of the hk reflections. Circles correspond to random orientation [equation (8d) or (15d)], solid line corresponds to the parallel case [equation (8b) or (15b)] and the crosses correspond to the cylindrical orientations [equations (8c) or (15c)].

graphitic lattice, with $2R=20 \text{ \AA}$ and bond length 1.42 \AA .

Lattice sum method

In principle, the lattice sum method involves the evaluation of

$$I(h, r) = \langle \exp [i(\mathbf{h} - \mathbf{h}_0) \cdot \mathbf{r}] \rangle$$

where \mathbf{r} is an inter-unit-cell distance vector and \mathbf{h}_0 is the reciprocal lattice vector defining the hkl reflection considered. The magnitude of \mathbf{h}_0 is $h_0 = 2\pi/z$, z being the spacing between the reflecting planes or lines. In employing this method, the intensity is expressed as a product of a unit-cell interference function, F^2 , and the lattice interference function, G^2 . The basic premise in deriving a valid analytical expression for the peak profile is that F^2 is more or less invariant in the region of h where G^2 gives rise to a peak. This is permissible if the number of unit cells in the structure is larger by a factor ten or more than the number of atoms in the unit cell.

The vector \mathbf{h}_0 is independent of the vector \mathbf{h} and for the two-dimensional hk reflections \mathbf{h}_0 lies in the layer; we have, therefore,

$$\langle \exp [i(\mathbf{h} - \mathbf{h}_0) \cdot \mathbf{r}] \rangle = \langle \exp (i\mathbf{h}_0 \cdot \mathbf{r}) \rangle \langle \exp (i\mathbf{h} \cdot \mathbf{r}) \rangle.$$

If the layers are random in rotation about their normals and random in translation we have

$$\langle \exp (i\mathbf{h}_0 \cdot \mathbf{r}) \rangle = J_0(h_0 r).$$

The average value of $\exp (i\mathbf{h} \cdot \mathbf{r})$ depends upon the type of preferred orientation and is essentially given by equations (2). Designating them by $I(h, r)$, the interference function takes the form

$$j(h) = \sum_{-\infty}^{\infty} g(r_q) J_0(h_0 r_q) I(h, r_q). \quad (9)$$

For the defective lattice $g(r)$ is given by $\exp(-ar)$ (Ergun, 1970a). Since the intensity is appreciable for small values of $h-h_0$, the necessary summation in equation (9) can be replaced by an integral over r and we may write

$$j(h) = \int_0^{\infty} \exp(-ar) 2\pi r \rho J_0(h_0 r) I(h, r) dr. \quad (10)$$

For the two-dimensional hk reflections ρ is defined from

$$\rho = mF^2/4A \quad (11)$$

m being the multiplicity of the reflections studied, F^2 , the structure factor and A is the area of the two-dimensional unit cell. Substituting equations (2) into (10) we obtain

$$j(h) = 2\pi \rho \int_0^{\infty} r \exp(-ar) J_0(h_0 r) \times J_0\left(hr \cos^2 \frac{\psi}{2}\right) J_0\left(hr \sin^2 \frac{\psi}{2}\right) dr \quad (12a)$$

$$j(h) = 2\pi \rho \int_0^{\infty} r \exp(-ar) J_0(h_0 r) J_0(hr) dr \quad (12b)$$

$$j(h) = 2\pi \rho \int_0^{\infty} r \exp(-ar) J_0(h_0 r) J_0^2(hr/2) dr \quad (12c)$$

$$j(hr) = (2\pi \rho / h) \int_0^{\infty} \exp(-ar) J_0(h_0 r) \sin(hr) dr. \quad (12d)$$

Equations (12) are integrated using Laplace and Hankel transforms. Equations (12a) and (12c) involve the product of three Bessel functions and can be reduced to the product of two Bessel functions using the relation (Heaviside, 1950).

$$J_0\left[\frac{u}{2}(b-a)\right] J_0\left[\frac{u}{2}(b+a)\right] = \frac{2}{\pi} \int_a^b \frac{J_0(ux) x dx}{\sqrt{b^2-x^2} \sqrt{x^2-a^2}}.$$

Equations (12a) and (12c) take the forms, respectively

$$j(h) = 4\rho \int_0^{\pi/2} \int_0^{\infty} r \exp(-ar) J_0(h_0 r) J_0(hr) \times (1 - \sin^2 \psi \sin^2 \alpha)^{1/2} dr d\alpha, \quad (13a)$$

$$j(h) = 4\rho \int_0^{\pi/2} \int_0^{\infty} r \exp(-ar) J_0(h_0 r) J_0(hr \sin \alpha) dr d\alpha. \quad (13c)$$

Equation (12b) involves the integral (Luke, 1962)

$$\int_0^{\infty} x \exp(-ax) J_0(bx) J_0(cx) dx = \frac{2aE(z)}{\pi \sqrt{a^2 + (b+c)^2}} \frac{1}{a^2 + (b-c)^2} \quad (14)$$

where E is the complete elliptical integral of the second kind and z is defined from

$$z^2 = 4bc/[a^2 + (b+c)^2]. \quad (14a)$$

Equation (12d) is readily integrable (Erdelyi, 1954). Using equations (13) and (14) and substituting $4\rho = mF^2/A$ we obtain

$$j(h) = \frac{mF^2}{A} \frac{E(z)a}{h_0} \int_0^{\pi/2} \frac{d\alpha}{(h\sqrt{1 - \sin^2 \psi \sin^2 \alpha} - h_0)^2 + a^2} \quad (15a)$$

$$j(h) = \frac{mF^2 a E(z)}{A [(h+h_0)^2 + a^2]^{1/2} [(h-h_0)^2 + a^2]} \quad (15b)$$

$$j(h) = \frac{mF^2}{A} \frac{E(v)}{2\sqrt{ah_0} \sqrt{h_0^2 + a^2}} F(x) \quad (15c)$$

$$j(h) = \frac{mF^2}{A} \frac{\pi}{4h\sqrt{ah}} F(y). \quad (15d)$$

Equations (15a-c) correspond to (12a-c) and to (8a-c) respectively.

In equations (15),

$$\begin{aligned} z^2 &= 4hh_0/[a^2 + (h+h_0)^2] \\ v^2 &= h^2/(a^2 + h^2) \end{aligned}$$

$$F(p) = \left(\frac{\sqrt{p^2+1} + p}{p^2+1} \right)^{1/2} \quad (16)$$

and x is defined by

$$x = (h^2 - h_0^2 + a^2)/2ah_0 \quad (16c)$$

and y is defined by

$$y = (h^2 - h_0^2 - a^2)/2ah. \quad (16d)$$

Equation (15a) is integrable; however, the resulting expression is cumbersome. Using a computer, the intensity profile can easily be calculated.

Equation (15b) can further be simplified. Generally $R > 5$ and $h_0 \neq 0$, and $E(z) \simeq 1.0$ and $(h+h_0)^2 + a^2$ can be replaced by $4h_0^2$ because the intensity only becomes significant when $h \rightarrow h_0$. With these simplifications it takes the form

$$j(h) = \frac{mF^2}{2Ah_0} \frac{a}{(h-h_0)^2 + a^2}. \quad (17b)$$

Equation (17b) has the Cauchy form. The peak height is given by

$$j(h_0) = mF^2 R / 2Ah_0.$$

The intensity is one-half the maximum when

$$h = h_0 \pm 1/R,$$

and the line width at half peak intensity is given by

$$\Delta h = 2/R.$$

A simple approach to derive similar equations is as follows. Since we are interested in obtaining the intensity profile of a given hk reflection corresponding to a spacing z , we are concerned with diffracting lines instead of diffracting planes. We may consider an element of area $z (= 2\pi/h_0)$ in extent along \mathbf{h}_0 and infinite in extent perpendicular to \mathbf{h}_0 and use it as a repeating unit. From the defective lattice theory we obtain for the 00 reflections

$$\begin{aligned} \frac{1}{\pi} \int_0^\infty \int_0^\pi \exp(-x/R) qz \exp(ix \cos \alpha) dx d\alpha \\ = 2\pi q / h_0 \sqrt{h^2 + a^2}. \end{aligned}$$

The interference function of the diffracting lines is given by (Ergun, 1970)

$$\begin{aligned} 1 + 2 \sum_0^\infty \exp(-qz/R) \cos(qhz) \\ \simeq (h_0/\pi R) / [a^2 + (h-h_0)^2]. \end{aligned}$$

The layer interference function is simply the product of the two expressions obtained, *i.e.*

$$j(h) = (2qa/\sqrt{h^2 + a^2}) / [a^2 + (h-h_0)^2].$$

With $4q = mF^2/A$, the above equation and equation (15b) substantially yield the same profile.

In deriving equation (15c), $(h \sin \alpha + h_0)^2 + a^2$ was replaced by $4h_0^2$ because the main contribution from the Cauchy function comes as $h \rightarrow h_0$ and $\sin \alpha \rightarrow 1$. The effect of this simplification was also found to be negligible by a numerical comparison of equation (15c) with (8c) as shown at the top of Fig. 3. The crosses correspond to the results of equation (15c). Equation (15d) involves no approximation. It has been checked numerically with results obtained from (8d); the comparison is shown in Fig. 3 (middle curve).

Equations (15c) and (15d) are governed by the function F defined by equation (16). The function has a maximum at $p = 1/\sqrt{3}$, and $F_{\max} \simeq 1.14$. The shift in peak position $h_{\max} - h_0$ is given by

$$h_{\max} - h_0 = 1/R\sqrt{3}.$$

Although equations (15c) and (15d) appear to be similar, they differ, especially on the high angle side, because of the differences in x and y and in the coefficients of $F(x)$ and $F(y)$.

The 00 reflections

These reflections are prominent when $h \rightarrow 0$ and are important in the analysis of small angle X-ray scattering. They are also important in the analysis of the 00 l reflections from the layered structures since the latter are produced by the modulation of the 00 re-

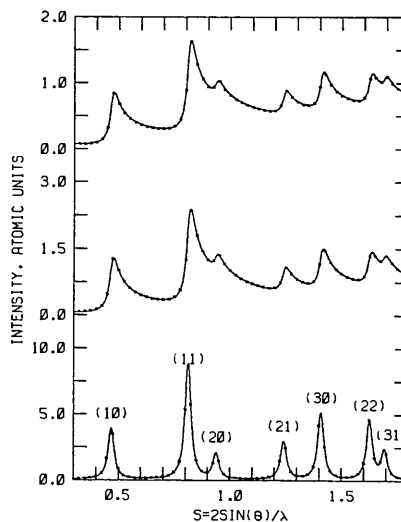


Fig. 3. Comparison of profiles calculated using interatomic sum method (solid line) and lattice sum method (crosses). The figure at the bottom corresponds to equations (8b) and (15b) (parallel case), the figure at the middle to equations (8d) and (15d) (random case), and the figure at the top to (8c) and (15c) (cylindrical case). From all of the equations, the 00 reflections have been excluded and in computing the profiles using the lattice sum technique the influence of 10 consecutive reflections has been included.

flections. For the 00 reflections $mF^2/A=4\rho$ and $h_0=0$; from equations (15b-d) we obtain, for the 00 reflections

$$j(h) = 2\pi\rho a/(h^2 + a^2)^{3/2} \quad \text{parallel case} \quad (18b)$$

$$j(h) = 4\rho E(v)/a(h^2 + a^2)^{1/2} \quad \text{cylindrical case} \quad (18c)$$

$$j(h) = 2\pi\rho/(h^2 + a^2) \quad \text{random case} \quad (18d)$$

where v is now defined by $v = h/\sqrt{h^2 + a^2}$.

At $h=0$, all of the above equations become identical, viz. $2\pi\rho R^2$. At $h \gg 1/R$, the above equations take the forms

$$j(h) = 2\pi\rho/Rh^3 \quad \text{parallel case} \quad (19b)$$

$$j(h) = 4\pi E(v)R/h \quad \text{cylindrical case} \quad (19c)$$

$$j(h) \simeq 2\pi\rho/h^2 \quad \text{random case.} \quad (19d)$$

From an inspection of equations (19) we note very important differences in the 00 reflections. In the parallel case it diminishes with $1/Rh^3$. Hence they essentially have no influence on the other reflections. For the random case $j(h)$ is more or less independent of R and decreases with $1/h^2$. For the cylindrical case at large values of h , $E(v) \rightarrow 1$, and the 00 reflections are proportional to R and diminish slowly, i.e. with $1/h$.

It may be pointed out that the intensities of the 00 reflections follow more simply from

$$j(h) = \int_0^\infty 2\pi\rho \exp(-ar) J_0(hr) dr \\ = 2\pi\rho a/(h^2 + a^2)^{3/2} \quad (20b)$$

$$j(h) = \int_0^\infty 2\pi\rho \exp(-ar) J_0^2(hr/2) dr \\ = 4\rho E(v)/a\sqrt{h^2 + a^2} \quad (20c)$$

$$j(h) = \int_0^\infty 2\pi\rho \exp(-ar) \sin(hr)/hr dr \\ = 2\pi\rho/(h^2 + a^2) \quad (20d)$$

For the general case we have

$$j(h) = \int_0^\infty 2\pi\rho \exp(-ar) J_0\left(hr \cos^2 \frac{\psi}{2}\right) \\ \times J_0\left(hr \sin^2 \frac{\psi}{2}\right) dr \\ = 4\rho a E(u)/[(h^2 \cos^2 \psi + a^2)\sqrt{h^2 + a^2}] \quad (20a)$$

where

$$u = h \sin \psi / \sqrt{h^2 + a^2}$$

and E is the complete elliptical function of the second kind.

In using equation (17b) i.e. the parallel case, the 00 reflections need not be considered and neighboring peaks have very little influence on any peak. These observations follow from an inspection of Figs. 2 and 3.

Comparison of equations (8d) and (15d) is shown in Fig. 3, middle. In the illustration, $2\pi\rho/(h^2 + a^2)$ has been subtracted from equation (8d) (solid line) and in the calculation of the curve shown by crosses, the 00 reflections have been excluded and the influence of ten consecutive peaks (3 not shown) is included. The identity is obvious. It is also clear that in calculating the profile in the vicinity of any peak, contributions of all of the peaks to the left need be included; three peaks to the right appear to be sufficient.

Comparison of equations (8c) and (15c) is also shown in Fig. 3 top. In the illustration $4\rho E(v)R/\sqrt{h^2 + 1/R^2}$ has been subtracted from equation (11c), solid line, and in the calculation of the crosses, the 00 reflections have been omitted and 10 consecutive peaks have been included (3 not shown). Although $E(v) \simeq 1.005$ at $h \simeq 2$ for $R=10$, the simplification $E(v) \simeq 1$ leads to serious error at the low-angle side of the 100 reflections.

References

- BACON, G. E. (1956). *J. Appl. Chem.* **6**, 477-478.
 BRAGG, L. & NYE, J. F. (1947). *Proc. Roy Soc.* **190**, 474-481.
 ERDELYI, A. (1954). Editor, *Tables of Integral Transforms*, Vol. II, p. 14. New York: McGraw-Hill.
 ERGUN, S. (1970a). *Phys. Rev.* **B1**, 3371-3380.
 ERGUN, S. (1970b). *Structural Studies of High Strength, High Modulus Graphite*. AFML-TR-69-51.
 ERGUN, S. (1970c). *J. Appl. Cryst.* **3**, 153-156.
 HEAVISIDE, O. (1950). *The Electromagnetic Theory*. p. 323. New York: Dover.
 LUKE, Y. L. (1962). *Integrals of Bessel Functions*. p. 316. New York: McGraw-Hill.
 RULAND, W. (1967). *J. Appl. Phys.* **38**, 3585-3589.
 WARREN, B. E. (1941). *Phys. Rev.* **59**, 693-698.
 WARREN, B. E. (1959). *Progress in Metal Physics*, Vol. 8. pp. 147-202. Edited by B. CHALMERS & R. KING. New York: Pergamon Press.